Published online 25 March 2013 *Nucleic Acids Research, 2013, Vol. 41, No. 9* ***4963–4975***
doi:10.1093/nar/gkt175

Distinctive contributions of the ribosomal P-site elements m^2G966, m^5C967 and the C-terminal tail of the S9 protein in the fidelity of initiation of translation in *Escherichia coli*

Smriti Arora[1], Satya Prathyusha Bhamidimarri[1], Moitrayee Bhattacharyya[2], Ashwin Govindan[1], Michael H. W. Weber[3], Saraswathi Vishveshwara[2] and Umesh Varshney[1,4,*]

[1]Department of Microbiology and Cell Biology, Indian Institute of Science, Bangalore 560012, India, [2]Molecular Biophysics Unit, Indian Institute of Science, Bangalore 560012, India, [3]Rechenkraft.net e.V., Chemnitzer Str. 33, D-35039 Marburg, Germany and [4]Jawaharlal Nehru Centre for Advanced Scientific Research, Bangalore 560064, India

Received February 10, 2013; Revised February 24, 2013; Accepted February 25, 2013

ABSTRACT

The accuracy of pairing of the anticodon of the initiator tRNA ($tRNA^{fMet}$) and the initiation codon of an mRNA, in the ribosomal P-site, is crucial for determining the translational reading frame. However, a direct role of any ribosomal element(s) in scrutinizing this pairing is unknown. The P-site elements, m^2G966 (methylated by RsmD), m^5C967 (methylated by RsmB) and the C-terminal tail of the protein S9 lie in the vicinity of $tRNA^{fMet}$. We investigated the role of these elements in initiation from various codons, namely, AUG, GUG, UUG, CUG, AUA, AUU, AUC and ACG with $tRNA^{fMet}_{CAU}$ ($tRNA^{fMet}$ with CAU anticodon); CAC and CAU with $tRNA^{fMet}_{GUG}$; UAG with $tRNA^{fMet}_{CUA}$; UAC with $tRNA^{fMet}_{GUA}$; and AUC with $tRNA^{fMet}_{GAU}$ using *in vivo* and computational methods. Although RsmB deficiency did not impact initiation from most codons, RsmD deficiency increased initiation from AUA, CAC and CAU (2- to 3.6-fold). Deletion of the S9 C-terminal tail resulted in poorer initiation from UUG, GUG and CUG, but in increased initiation from CAC, CAU and UAC codons (up to 4-fold). Also, the S9 tail suppressed initiation with $tRNA^{fMet}_{CUA}$ lacking the 3GC base pairs in the anticodon stem. These observations suggest distinctive roles of 966/967 methylations and the S9 tail in initiation.

INTRODUCTION

The accuracy of mRNA decoding is central to the fidelity of translation. Structural studies have revealed that during elongation, correct minor groove geometry of the base pairs formed by the first two nucleotides of the codon with the complementary nucleotides of the anticodon in the ribosomal A-site is scrutinized by A1492, A1493 and G530 of the 16S rRNA (1). In contrast, at the step of initiation, although it is clear that the correct pairing of the initiator tRNA ($tRNA^{fMet}$) anticodon with the initiation codon in the ribosomal P-site determines the translational reading frame in an mRNA, it is unclear how the pairing between the anticodon and the initiation codon is scrutinized. For example, $tRNA^{fMet}_{CAU}$ ($tRNA^{fMet}$ with CAU anticodon) initiates not only from AUG but also from GUG, UUG and CUG, interestingly, by allowing wobble/mismatch at the first position of the codon (unlike the third position wobble during elongation). Also, other than the special cases, such as AUU in *infC* (2) and AUA in mitochondria (3), it is unclear whether initiation *in vivo* occurs from codons with the third base wobbling/mismatch. Whether any A-site like mechanisms play a role in scrutinizing the interaction between the anticodon of $tRNA^{fMet}$ and the initiation codon of an mRNA in the P-site (at the step of initiation) is unknown.

High-resolution co-crystal structures of the 70S ribosome bound with $tRNA^{fMet}$ in the P-site (together with $tRNA^{Phe}$ bound in the A- and E-, sites) and an

*To whom correspondence should be addressed. Tel: +91 80 2293 2686; Fax: +91 80 2360 2697; Email: varshney@mcbl.iisc.ernet.in or uvarshney@gmail.com

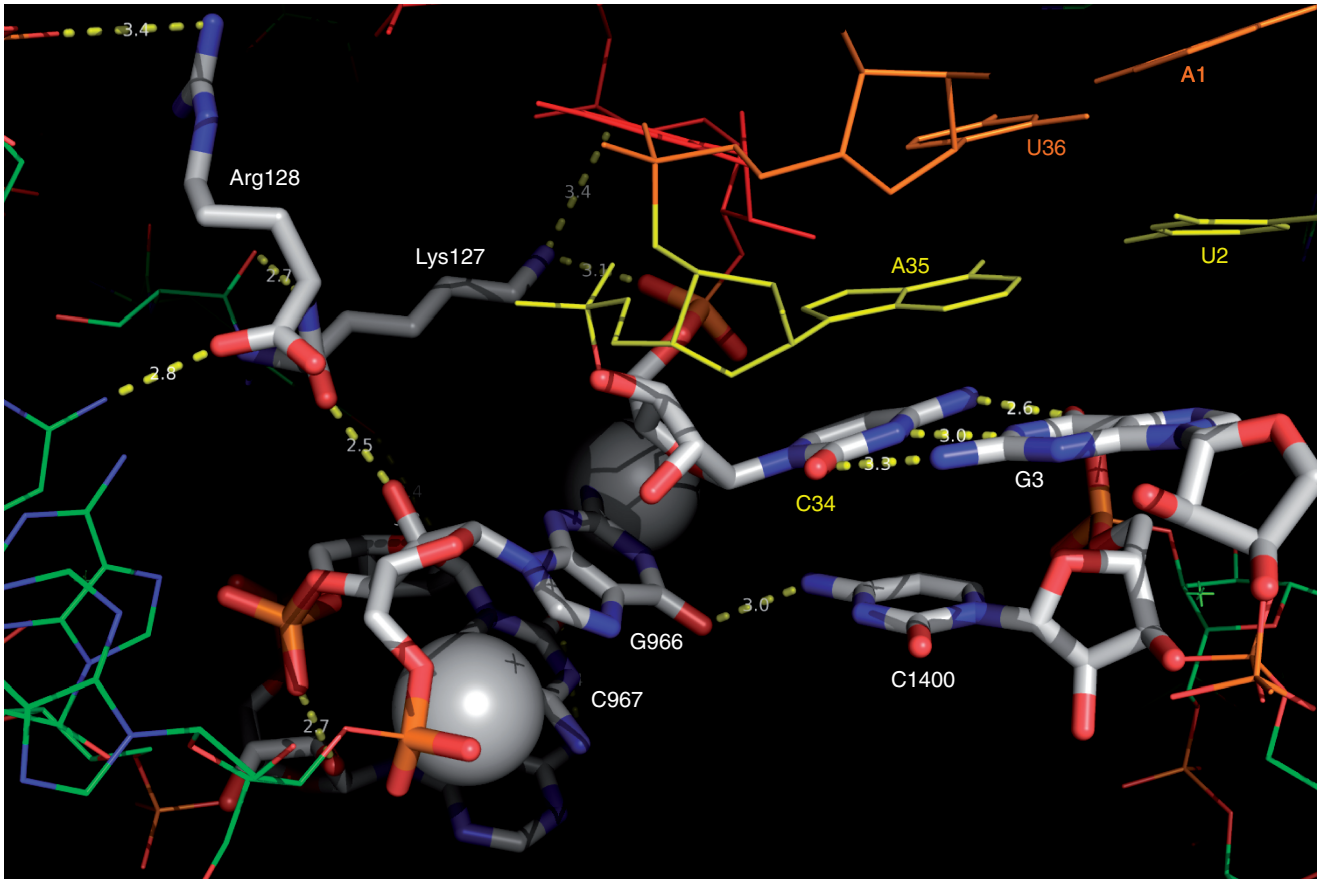

Figure 1. P-site model showing interaction of CAU anticodon (C34, A35 and U36) of $tRNA^{fMet}$ with AUG initiation codon (A1, U2 and G3). Contacts of G966, C967 and the S9 tail are shown. Spheres associated with G966 and C967 indicate methyl groups at their positions 2 and 5, respectively. Lys127 of S9 tail contacts C34 of the anticodon and is in proximity to G966 and C967. The model was generated with PyMOL v1.3r1 using PDB accession number 2J00 (4).

mRNA (4,5) yielded insights into the distinctive features of the P-site. A methylated nucleoside of the 16S rRNA, G966, stacks against the ribose of the first base of the anticodon (C34) of the $tRNA^{fMet}$. The residue C967, also a methylated nucleoside, lies next to G966 and is also in proximity to $tRNA^{fMet}$ (Figure 1). The G966 and C967 methylations are carried out by the specific methyltransferases, RsmD and RsmB, respectively (6,7). The structural data (4) have also revealed that the tail of S9 protein extends into the P-site and contacts $tRNA^{fMet}$ at positions 33 and 34 (Figure 1). The C-terminal tail sequence of the S9 protein is phylogenetically conserved (8). And, although modification of residue 966 is also conserved, neither the identity of the residue nor the nature of the modification is conserved (9,10). The residues G966 and C967 lie in the 970 loop, which forms helix 31, and mutation of either has been reported to result in a slight increase (107–127%) in production of a reporter protein (11). The C967 methylation is conserved in bacteria, and the two methylated nucleosides are also reported to contact the S9 tail via the backbone interactions (12,13), thus forming a network of interactions with $tRNA^{fMet}$ in the P-site. In recent years, roles of post-transcriptionally modified nucleosides have been studied by several groups, and methylated nucleosides have been shown to impact fidelity of initiation (14), ribosome recycling (15,16), ribosome biogenesis (17) and response to nascent peptide (18).

To investigate the role of methylations of the adjacent nucleotides G966 and C967 and the C-terminal tail of the ribosomal protein S9 in initiation, we deleted RsmB, RsmD and the last three amino acids of S9 (independently or together) from the *Escherichia coli* chromosome. The strains so developed were then used to study initiation from a variety of initiation codons with the native or mutant initiator tRNAs. We show that the S9 tail and the modified G966/C967 contribute to the correct poising of $tRNA^{fMet}$ in the ribosomal P-site in *E. coli*.

MATERIALS AND METHODS

Strains, plasmids and DNA oligomers

E. coli strains, plasmids and DNA oligomers used in this study are listed in Supplementary Tables S1–S3. Bacteria were cultured in Luria–Bertani broth (LB) or LB-agar (LB containing 1.8% agar, Difco) at 37°C or as indicated with constant shaking at 200 rpm. Ampicillin (Amp, 100 $\mu g\,ml^{-1}$), kanamycin (Kan, 25 $\mu g\,ml^{-1}$) or tetracycline (Tet, 7.5 $\mu g\,ml^{-1}$) were used as needed.

Generation of knockout and knockin strains

Details of the strains generated are provided in the Supplementary Material.

Generation of chloramphenicol acetyltransferase reporter constructs containing mutant initiation codons and the corresponding anticodon sequences in the initiator tRNA (encoded by *metY*)

Reporter constructs were derived from $pCAT_{AUG}metY$ or $pCAT_{UAG}metY_{CUA}$ (19) using two steps of site-directed mutagenesis to first mutate the initiation codon of the chloramphenicol acetyltransferase (CAT) reporter and then the anticodon sequence in the *metY* gene. Reactions (50 µl) contained ~100 ng DNA template, 200 µM dNTPs, 20 pmol of the required forward and reverse primers (Supplementary Table S3) and 1 U Phusion™ DNA polymerase (2 U µl^{-1}, Finnzymes). All constructs were verified by DNA sequencing.

Preparation of the cell-free extracts

E. coli strains were grown (3–5 replicates) in 3 ml of LB with Amp at 37°C to an OD_{600} of ~0.6–0.7. The cells were harvested, and the cell-free extracts were prepared, quantified and stored at −20°C (14).

CAT assays

CAT assays using the cell-free extracts (0.3–2.0 µg total protein) were performed in 30-µl reactions containing 500 mM Tris–HCl, pH 8.0, 150 µM chloramphenicol, 0.025 µCi (430 pmol) [^{14}C]-Cm (specific activity 57.8 m Ci mmol^{-1}; Perkin Elmer) and 432 µM acetyl-CoA at 37°C for 20 min followed by separation of the substrate and products by thin layer chromatography (15). The pixel counts were estimated for the spots corresponding to the substrate (S, chloramphenicol) and products (P, 1-acetyl and 3-acetyl chloramphenicol) using the Multi Gauge software. Per cent CAT activities were calculated as $[P/(S+P)] \times 100$. This value was divided by the amount of total protein (in micrograms) used for each assay. The activity so obtained was then normalized to the relative value of β-lactamase activity of the corresponding extract to avoid any variations in the CAT values because of plasmid copy number changes.

β-Lactamase assay

β-Lactamase assays in 125-µl volumes contained CENTA™ (0.2 mM, Calbiochem), a chromogenic substrate, and cell-free extracts (0.8–1.0 µg total proteins) for 30 min in 10 mM Tris–HCl (pH 8.0). The reaction was stopped by addition of 3 µl of 5% sodium dodecyl sulphate, and the volume was made up to 400 µl with water. Absorbance was measured at 405 nm. The value of *E. coli* SA extracts in each replicate was considered as unit, and the values of other extracts were calculated relative to this value.

Calculation of fold differences in CAT activities

CAT activities of 3–5 replicates were determined. Fold differences for the CAT values of all strains (i.e. *E. coli* SA and its derivatives) for each of the CAT constructs were calculated by dividing them with the corresponding value of the SA strain for each of the replicates. The averages of the fold differences for each strain were calculated and plotted along with SEM. Values for SA in such calculations remain as unit for each construct. The graphs plotted represent CAT activity per micrograms (normalized to its relative β-lactamase activity) of each strain relative to the control *E. coli* SA parent strain. A schematic of calculation of fold difference in CAT activity is given in Supplementary Figure S1. In all assays, a difference of ≥2-fold (with respect to the control) was considered significant.

Molecular dynamics simulations

Four codon:anticodon pairs, namely, the wild-type AUG:CAU, and an array of the mutants CAC:GUG, CAU:GUG and AUC:GAU were used for modelling and molecular dynamics (MD) simulations in the presence or absence of the S9 tail (the three C-terminal Ser126, Lys127 and Arg128, SKR, residues; the S9 tail deletion set is theoretically equivalent to the S9 protein being absent from the MD simulations). The region representing the mRNA:$tRNA^{fMet}$ complex in the presence of the S9 tail was carved out of the crystal structure of the ribosome (PDB accession number 2J00) from *Thermus thermophilus* (4). The corresponding structure of *E. coli* ribosome was not chosen because the *E. coli* structure is complexed with $tRNA^{Phe}$ instead of $tRNA^{fMet}$ (5). However, the region of our interest (i.e. P-site tRNA + mRNA + S9) shows high-structural similarity to *T. thermophilus* [Root Mean Square Deviation (RMSD): 1.05 Å]. The mutant pairs were generated using the 'mutate_bases' module in the 3 DNA package (20), followed by minimization, equilibration and MD simulations for 10 ns each. MD simulations were carried out in aqueous medium using TIP3P water model using the force field ff99.rna. Na^+ ions were added to each system to neutralize the net charges using tleap in AMBER9 (21). The solvation box is 14 Å from the farthest atom along any axis. The simulations were performed under normal pressure and temperature (NPT) conditions with the Berendsen temperature coupling scheme and periodic boundary conditions. Particle Mesh Ewald (PME) summation was used for long-range electrostatics. The van der Waals' cut-off used is 10 Å, and the pressure and temperature relaxations were set to 0.5 ps^{-1}. A time step of 2 fs was used with the integration algorithm, and the structures were stored every 1 ps. The trajectories from 1–10 ns were used for the hydrogen bond analysis. The hydrogen bonding analysis was done on each snapshot [distance cut-off for identifying hydrogen bonds (H-bonds) being 3.5 Å]. The H-bonds, which appear in >40% of the MD ensemble, were termed dynamically stable and were chosen for further analyses and inference.

RESULTS

In vivo system for initiation from different codon:anticodon pairs

The *in vivo* assay is based on a plasmid containing a CAT reporter gene (19) whose initiation codon (AUG) was

mutated to UAG, CAC, CAU, UAC, GUG, UUG, CUG, AUU, AUA, AUC or ACG. The initiator tRNA ($tRNA^{fMet}$) gene (*metY*) with a corresponding change in its anticodon (CAU) to CUA to decode UAG; GUG to decode CAC and CAU; GUA to decode UAC and GAU to decode AUC was also present on the same plasmid. The AUG, GUG, UUG, CUG, AUU, AUA, AUC and ACG codons were decoded by the native $tRNA^{fMet}_{CAU}$ (Supplementary Tables S4 and S5). The initiation activities of the CAT reporters were monitored by growth of the strains on chloramphenicol (Cm) plates, CAT assays or immunoblotting (22,23).

As anticodon (CAU) is the major determinant for aminoacylation of $tRNA^{fMet}$ by MetRS (24,25), mutations in anticodon (needed for initiation with many of the non-AUG codons) often result in aminoacylation of the mutant $tRNA^{fMet}$ with non-methionine amino acids (Supplementary Table S6). Although, in *E. coli*, initiation with a variety of non-methionine amino acids has been reported, their initiation efficiencies vary (26). Thus, to avoid any variations because of initiating amino acids, the CAT activities were used only to determine the ratios (fold differences) of initiation between the strain deficient for the specific ribosomal P-site feature(s) versus the control strain (wild-type for the same ribosomal P-site features) independently for each of the codon:anticodon pair. It may also be said that as in our assay design, only the initiation codon of the reporter and/or the anticodon of the initiator tRNA are changed, the assay reports specifically on the impact of the ribosomal P-site elements on initiation.

Use of initiator tRNAs with GUG or QUG anticodons

The native $tRNA^{fMet}$ with CAU anticodon possesses cytosine, a pyrimidine, at position 34. To address whether a purine at this position, such as in GUG or QUG codons [where Q represents queuosine, a bulky modification of guanosine found in tRNAs with GUN anticodon, (27)], could be allowed, we introduced the reporter $pCAT_{CAC}metY_{GUG}$ into *E. coli* BW and its Δ*tgt*::*kan* derivative referred to as *E. coli* SA or SA (deficient in Tgt, which is required for Q modification). *E. coli* BW and *E. coli* SA served to study initiation with $tRNA^{fMet}_{QUC}$ and $tRNA^{fMet}_{GUG}$, respectively. The tRNAs encoded by $metY_{GUG}$ are novel variants that initiate, but the amino acid attached to these has not been identified. As shown in Supplementary Figures S2–S4,

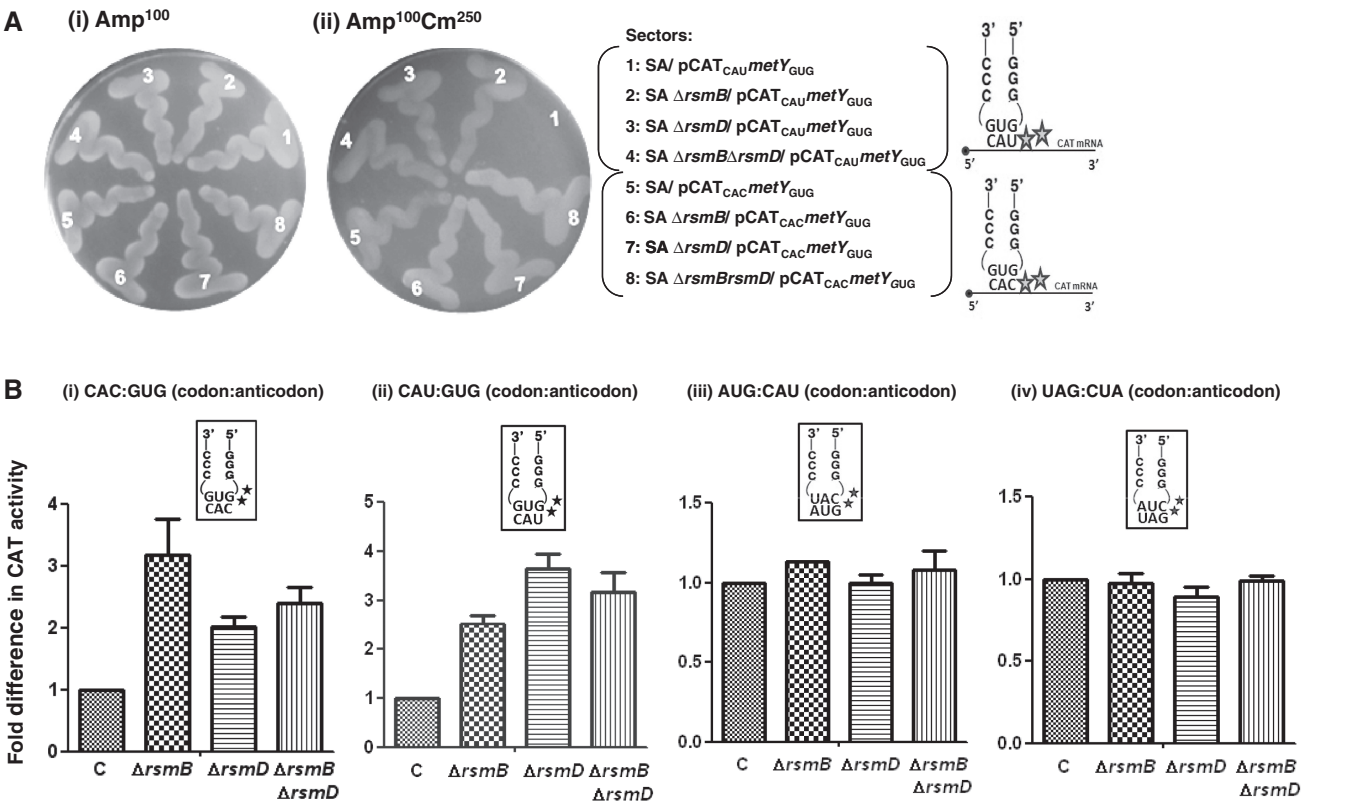

Figure 2. Initiation from CAC and CAU codons by $tRNA^{fMet}_{GUG}$ (encoded by $metY_{GUG}$) as assessed by growth on Cm plate (**A**). Saturated cultures of *E. coli* SA and its Δ*rsmB*, Δ*rsmD*, and Δ*rsmB* Δ*rsmD* derivatives harbouring $pCAT_{CAU}metY_{GUG}$ (sectors 1–4) or $pCAT_{CAC}metY_{GUG}$ (sectors 5–8) were streaked on Amp^{100} (left) or Amp^{100} Cm^{250} (right) and incubated at 37°C for ~15 h. CAT assays (**B**) to assess initiation activities of CAC:GUG (panel i), CAU:GUG (panel ii), AUG:CAU (panel iii) and UAG:CUA (panel iv) codon:anticodon pairs. Star symbols in the boxes indicate G966 (anticodon proximal) and C967. Fold differences in the CAT activities with respect to SA (C, taken as 1) in its Δ*rsmB*, Δ*rsmD*, and Δ*rsmB* Δ*rsmD* derivatives are shown. For reference, the average CAT activities in SA (C) for the CAC:GUG, CAU:GUG, AUG:CAU and UAG:CUA codon:anticodon pairs were 1462 ± 374, 493 ± 64, 7314 ± 923 and 5246 ± 763 pmol Cm acetylated per 1 μg of total cell-free extract in 20 min at 37°C, respectively.

although the *metY*$_{GUG}$ encoded tRNA^{fMet} was queuosinylated in *E. coli* BW and it participated in initiation, to avoid complications because of its partial modification, *E. coli* SA was used to investigate initiation with tRNA$^{fMet}_{GUG}$ and all other tRNAs.

Methylated G966 and C967 suppress initiation with tRNA$^{fMet}_{GUG}$

The pCAT$_{CAC}$*metY*$_{GUG}$ and pCAT$_{CAU}$*metY*$_{GUG}$ constructs were introduced into *E. coli* SA and its derivatives to measure initiation from CAC:GUG and CAU:GUG codon:anticodon pairs, respectively. Transformants were grown in LB with Amp and streaked on LB-agar containing 100 μg ml^{-1} Amp (Amp^{100}) as control and on LB-agar Amp^{100} with varying concentrations of Cm (Amp^{100} Cm$^{100-250}$). Representative plates with Amp^{100} or Amp^{100} Cm^{250} (Figure 2A) show that the pCAT$_{CAU}$ *metY*$_{GUG}$ supported the growth of the strains deleted for methyltransferases in singles (Δ*rsmB* or Δ*rsmD*) or double (Δ*rsmB* Δ*rsmD*) (sectors 2–4) but not of the parent (sector 1), suggesting better initiation by tRNA$^{fMet}_{GUG}$ in the absence of methylations at positions 966 and/or 967. In the plate assay, the transformants harbouring pCAT$_{CAC}$*metY*$_{GUG}$ (sectors 5–8) did not show a perceivable difference in growth (because of higher level of initiation from the matched CAC codon). However, as revealed by the CAT assays (Figure 2B, panels i and ii), deletion of methyltransferases in singles or double resulted in increased initiation by tRNA$^{fMet}_{GUG}$ (~2- to 3.6-fold) over the SA parent (C) from both CAC and CAU codons (see also Supplementary Figure S6). Interestingly, as shown in Figure 2B (panels iii and iv), the deficiency of these methyltransferases showed no significant changes in initiation with AUG (decoded by native tRNA$^{fMet}_{CAU}$) or UAG (decoded by near native tRNA$^{fMet}_{CUA}$).

Methylated G966 suppresses initiation from AUA codon

Deletion of *rsmD* resulted in increased initiation with the CAU:GUG pair (U:G mismatch at the third position of codon) to a level (>3-fold) that was higher than that seen for the perfectly matched pair CAC:GUG (~2-fold) (Figure 2B). This led us to investigate whether G966 methylation discriminated against the third position (of the initiation codon) wobble/mismatch. To address this, initiation from various canonical codons AUG, GUG, UUG (28) and CUG (29) and non-canonical codons AUU (2), AUA (30), AUC and ACG with the native initiator tRNA (Supplementary Table S4) was investigated. As seen in Figure 3, on deletion of *rsmD*, initiation from AUA (third base mismatch with

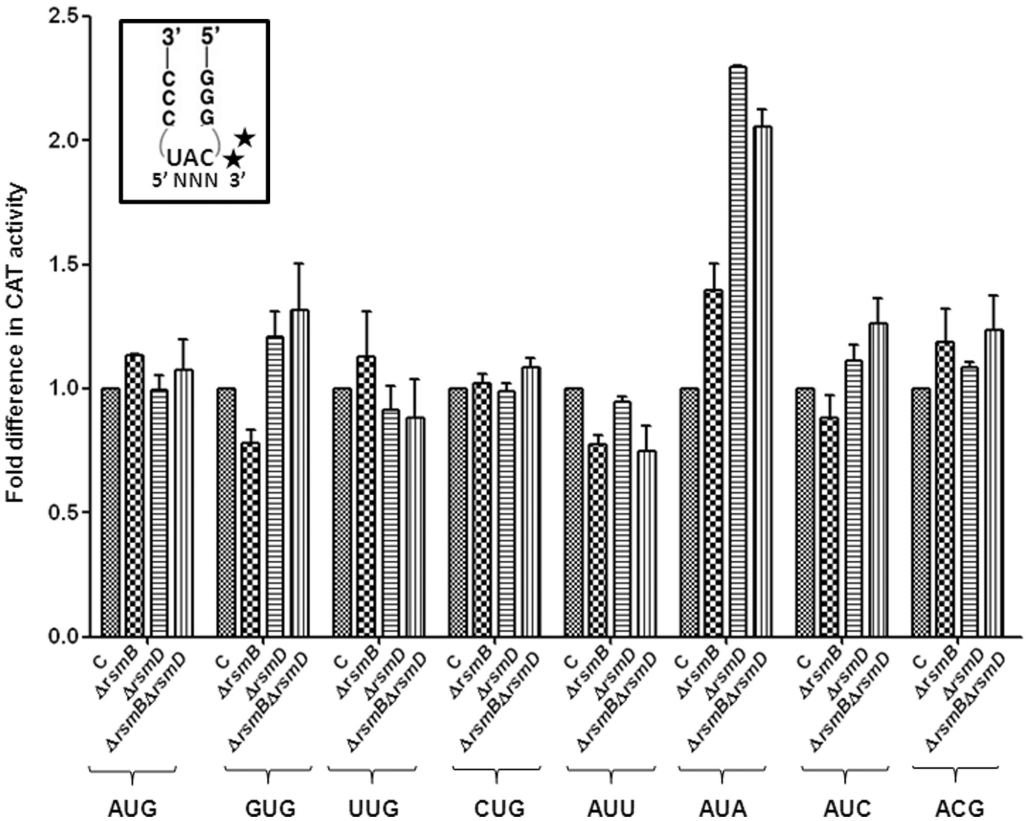

Figure 3. Initiation activities of the native tRNA$^{fMet}_{CAU}$ from various codons. Star symbols in the box indicate G966 (anticodon proximal) and C967. Fold differences in the CAT activities with respect to SA (C, taken as 1) in its Δ*rsmB*, Δ*rsmD*, and Δ*rsmB* Δ*rsmD* derivatives are shown. For reference, the average CAT activities in the SA control (C) for the AUG, GUG, UUG, CUG, AUA, AUU, AUC and ACG constructs were 7314 ± 923, 3629 ± 492, 4019 ± 1000, 906 ± 132, 238 ± 33, 301 ± 32, 352.5 ± 38 and 48 ± 15 pmol Cm acetylated per 1 μg of total cell-free extract in 20 min at 37°C, respectively.

$tRNA^{fMet}_{CAU}$) was at an advantage (~2-fold), but initiation from the remaining codons was not impacted significantly. Also, deletion of *rsmB* (alone or in combination with *rsmD*) did not have much impact.

Generation of the S9 C-terminal tail deletion strains

The C-terminal sequence (Ser126, K127 and R128, or SKR) of the ribosomal protein S9 is conserved, and the last two of these contact positions 33 and 34 of $tRNA^{fMet}$ (4). Lys127 is also in proximity to the methylated nucleosides G966 and C967 (Figure 1). This prompted us to investigate whether the C-terminal tail of the S9 protein contributes to decoding/fidelity at the step of initiation. A strain, S9Δ3, was generated wherein the C-terminal SKR sequence of S9 was deleted to disrupt its contacts with $tRNA^{fMet}$ (Supplementary Material). As shown in Supplementary Figure S7A, although the S9Δ3 strain and its derivatives, Δ*rsmD* S9Δ3, Δ*rsmB* S9Δ3, and Δ*rsmB* Δ*rsmD* S9Δ3, are cold sensitive, they grow normally at 37°C.

S9 tail suppresses initiation from unnatural codon:anticodon pairs

E. coli SA and its derivatives were transformed with $pCAT_{CAC}metY_{GUG}$, $pCAT_{CAU}metY_{GUG}$, $pCAT_{AUG}$ or $pCAT_{UAG}metY_{CUA}$ and used to monitor initiation (Figure 4). Initiation from the unnatural codons, CAC and CAU, using $tRNA^{fMet}_{GUG}$ showed ~3- to 4-fold increase in initiation in S9Δ3 and S9Δ3 Δ*rsmD* strains (panels i and ii). However, initiation from AUG using $tRNA^{fMet}_{CAU}$ or from UAG using a near natural $tRNA^{fMet}_{CUA}$ (panels v and vi) showed no significant changes. Combining *rsmD* deletion

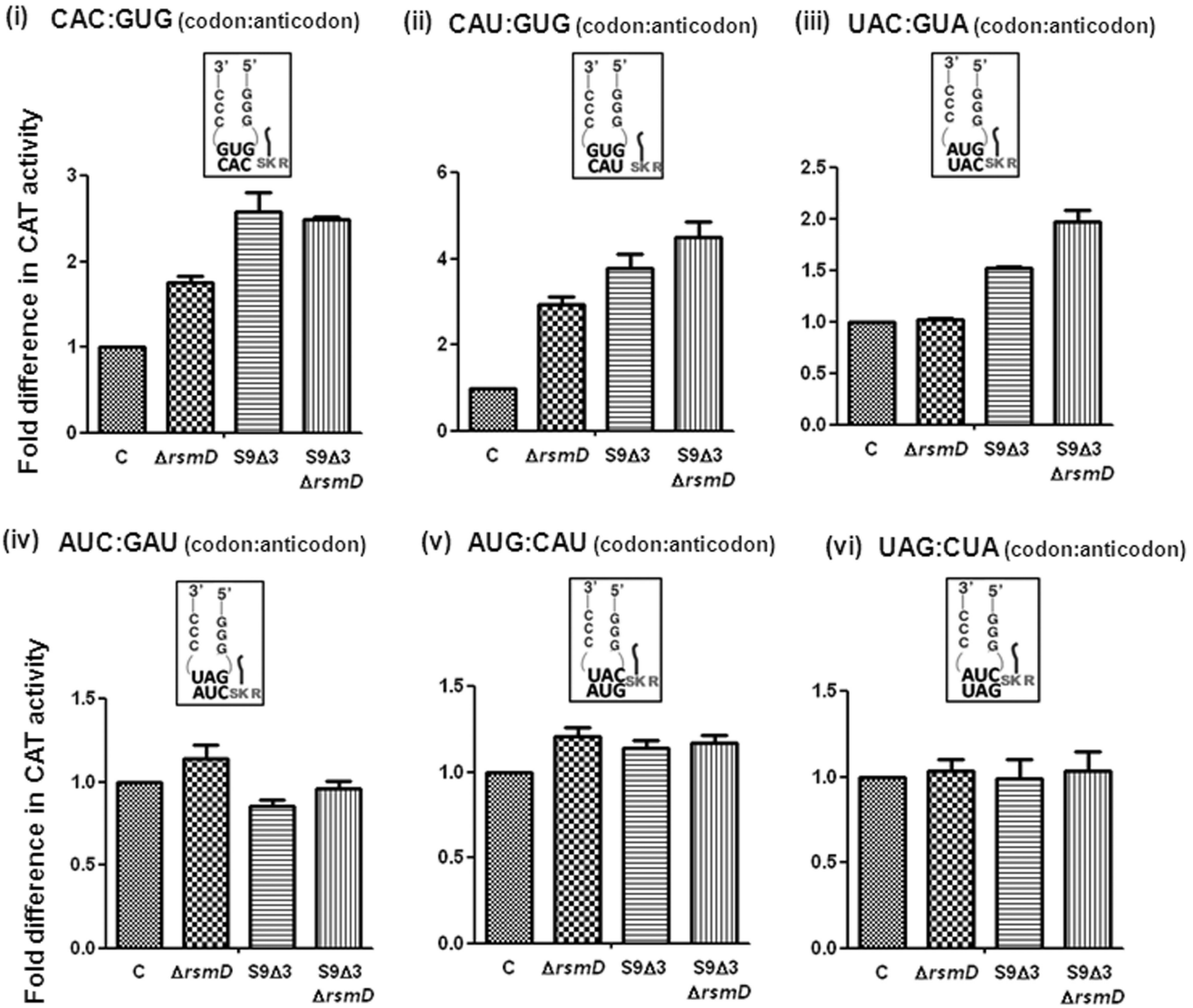

Figure 4. Initiation with CAC:GUG (panel i), CAU:GUG (panel ii), UAC:GUA (panel iii), AUC:GAU (panel iv), AUG:CAU (panel v) and UAG:CUA (panel vi) codon:anticodon pairs. A tail ending in SKR indicates ribosomal protein S9. Fold differences in the CAT activities with respect to SA (C, taken as 1) in its Δ*rsmD*, S9Δ3, and S9Δ3 Δ*rsmD* derivatives are shown. For reference, the average CAT activities in SA (C) for the CAC:GUG, CAU:GUG, UAC:GUA, AUC:GAU, AUG:CAU and UAG:CUA constructs were 1236 ± 151, 590 ± 103, 241 ± 26, 12266 ± 2866, 7838 ± 610 and 5454 ± 682 pmol Cm acetylated per 1 μg of total cell-free extract in 20 min at 37°C, respectively.

with S9Δ3 (Δ*rsmD* S9Δ3) did not increase initiation any significantly (Figure 4).

S9 tail deletion increases initiation with UAC:GUA but not with AUC:GAU codon:anticodon pairs

To investigate whether the S9 tail disfavoured other unnatural codon:anticodon pairs, initiation from UAC by $tRNA^{fMet}_{GUA}$ and AUC by $tRNA^{fMet}_{GAU}$ (26) was examined. Although in our assays, a steady-state accumulation of the formylated form of $tRNA^{fMet}_{GAU}$ and both the formylated and aminoacylated forms of $tRNA^{fMet}_{GUA}$ were undetectable (Supplementary Figure S8), both of these tRNAs initiated, suggesting that the respective forms must be used as soon as they are generated. Interestingly, the CAT assays revealed that deletion of the S9 tail resulted in a subtle increase in initiation from UAC (~1.5-fold); and a combined deletion of the S9 tail and *rsmD* resulted in ~2-fold increase in initiation (Figure 4, panel iii), suggesting that S9 tail discriminates against the codon:anticodon pairs unnatural to initiation. An initiation assay was also done with AUC using $tRNA^{fMet}_{GAU}$, a perfectly matched pair (panel iv). Here, deletion of S9 tail did not change initiation (~0.8-fold, Figure 4). This seemed to be an exception (see later in the text for analysis of dynamically stable H-bonds). In addition, this codon:anticodon pair (AUC:GAU) also suffered a problem because of background initiation from AUC using the native $tRNA^{fMet}_{CAU}$ (Figure 3).

S9 tail deletion decreases initiation from the less frequently used alternate initiation codons (UUG and GUG)

Alternate initiation codons GUG, UUG and CUG with a mismatch at the first codon position are not uncommon in mRNAs and are decoded by the native $tRNA^{fMet}_{CAU}$. CAT reporters that initiate from these codons showed that although the S9 tail deletion did not impact initiation from AUG, it led to a decrease in initiation from GUG, UUG and CUG (Figure 5). In the absence of the S9 tail, the mismatched codon:anticodon pairs may be less stable, and the tail may be required to maintain interactions between the anticodon and the codon with first base wobble/mismatch. Initiation from ACG; and AUA, AUC, and AUU with the native $tRNA^{fMet}_{CAU}$ (mismatches at the second or the third positions of the codon) showed that these activities remained unchanged in the S9Δ3 strain (Figure 5).

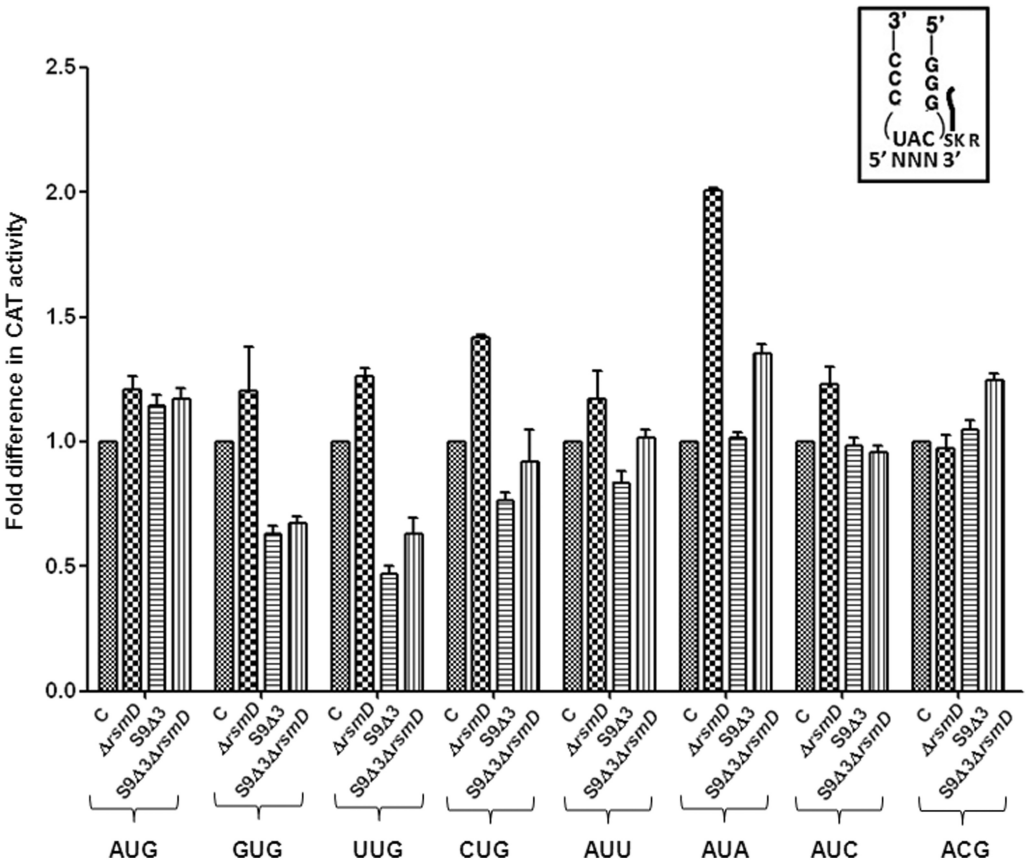

Figure 5. Initiation in absence of the S9 tail alone or in combination with deletion of *rsmD* with various initiation codons using the native initiator tRNA ($tRNA^{fMet}_{CAU}$). A tail ending with SKR in the box on the top right indicates ribosomal protein S9. Fold differences in the CAT activities with respect to SA (C, taken as 1) in its Δ*rsmD*, S9Δ3, and S9Δ3 Δ*rsmD* derivatives are shown. For reference, the average CAT activities in SA strain (C, taken as 1) for the AUG, GUG, UUG, CUG, AUA, AUU, AUC and ACG constructs were 7838 ± 610, 3198 ± 378, 3788 ± 334, 327 ± 15, 313 ± 19, 346 ± 34, 631 ± 71.6 and 78 ± 9 pmol Cm acetylated per 1 μg of total cell-free extract in 20 min at 37°C, respectively.

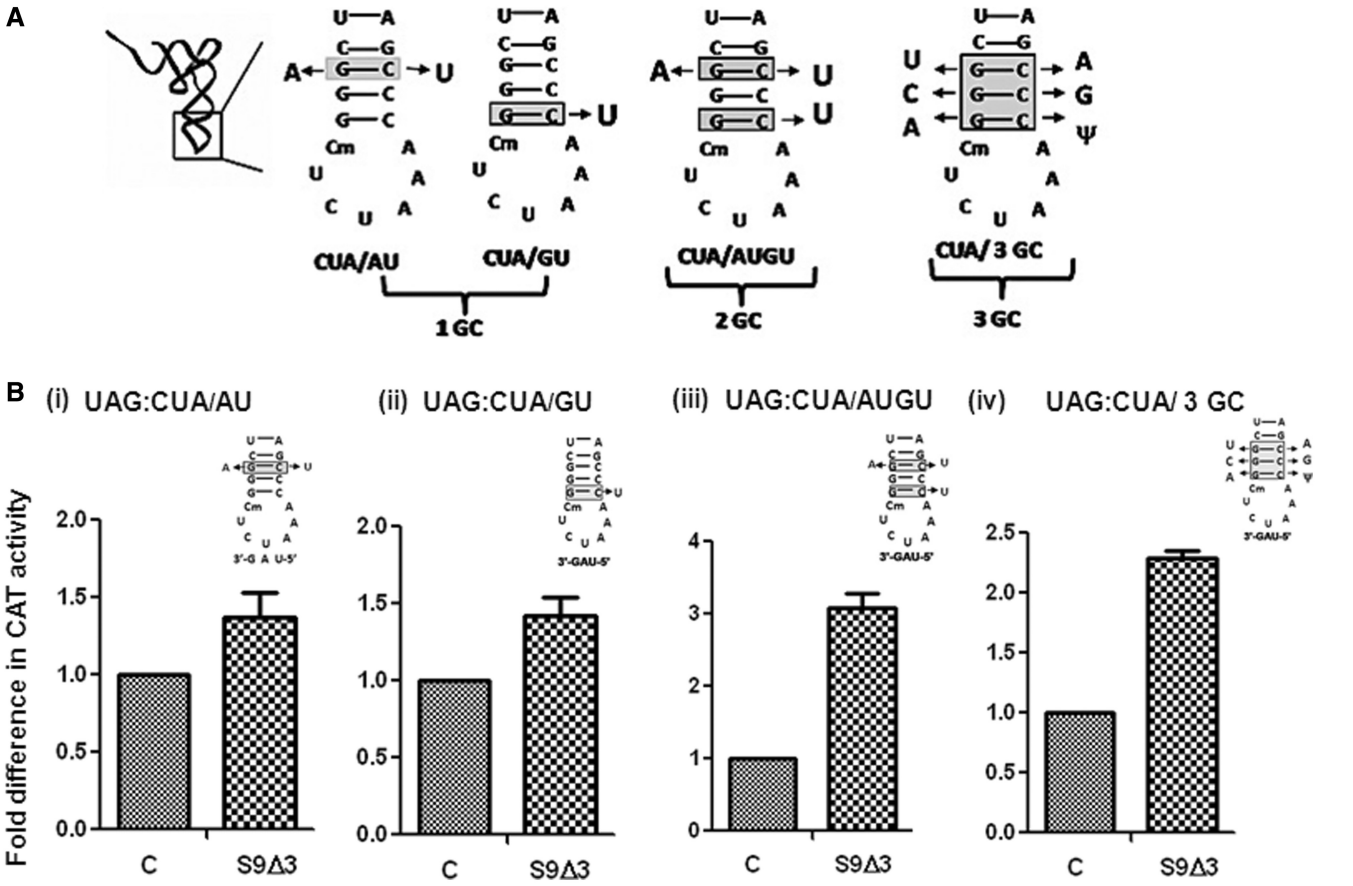

Figure 6. Effect of deletion of the S9 tail on initiation with the anticodon stem mutants of $tRNA^{fMet}_{CUA}$. Various mutations in the anticodon stem are as shown (**A**). Fold differences in the CAT activities with respect to SA (C, taken as 1) in its S9Δ3 derivatives are shown (**B**) for 1GC (AU, panel i), 1GC (GU, panel ii), 2GC (AU/GU, panel iii) and the 3GC mutant (panel iv). For reference, the average CAT activities in SA for the UAG:CUA/AU, UAG:CUA/GU, UAG:CUA/AUGU and UAG:CUA/3GC constructs were 2970 ± 900, 888 ± 145, 32 ± 6, 238 ± 33 and 88 ± 19 pmol Cm acetylated per 1 μg of total cell-free extract in 20 min at 37°C, respectively.

S9 tail deletion affords better initiation with the 2GC and 3GC mutants of $tRNA^{fMet}$

The S9 tail is flexible, and we hypothesized that it may sense alterations in the conformation of the anticodon arm of the initiator tRNA. To investigate whether the S9 tail imposes any preference for the $tRNA^{fMet}$ via its highly conserved feature of the three consecutive GC (3GC) base pairs in the anticodon stem, we used $tRNA^{fMet}$ mutants (Figure 6A) possessing changes at the first, first and third, third or all 3GC base pairs (15,31). The CAT reporters were introduced into *E. coli* SA and its S9Δ3 derivative. As expected from our earlier observation (Figure 4, panel vi), the initiation activity of $tRNA^{fMet}_{CUA}$ (with 3GC base pairs intact) from UAG did not change on deletion of the S9 tail. However, the initiation activities of the 2GC and the 3GC variants (A:U/G:U and 3GC; Figure 6B, panels iii and iv) showed an increase of >2-fold. The increases in initiation by the 1GC mutants, not unexpectedly, were subtle (Figure 6, panels i and ii).

MD simulations

The MD simulations of AUG:CAU, CAC:GUG and CAU:GUG codon:anticodon pairs with or without the S9 tail did not exhibit any drastic conformational changes at the backbone level of $tRNA^{fMet}$. However, a rigorous H-bond analysis along the trajectory provided excellent means of capturing subtle conformational re-orientations, taking into account the minor rewiring at the side-chain level. The AUG:CAU pair exhibits a dynamically stable H-bond (indicated by blue line, Figure 7, panel i) with the S9 tail, which exists in >70% of the snapshots. Another H-bond (indicated by yellow line) was observed in fewer (~57%) snapshots. Of these, the one indicated in blue was also reported in crystal structure of the initiator tRNA ribosome complex (4). The deletion of the S9 tail (leading to loss of these weak H-bonds) is expected to show no major effects on the interaction of native anticodon (CAU) with the AUG initiation codon. In the CAC:GUG codon:anticodon pair, substitution of C34 anticodon position by G34 affects subtle conformational variations during dynamics, which induced enhanced H-bonding of the tRNA with the S9 tail (Figure 7, panel ii). These H-bonds arrest the intrinsic dynamics and have a freezing effect on the tRNA, which is released on the S9 tail deletion. Thus, the S9 tail deletion is proposed to allow the tRNA regain the conformational dynamics important for efficient recognition of the CAC

initiation codon. As shown in Figure 7, panel iii, for the CAU:GUG codon:anticodon pair, along with the mutation at the 34 position of the anticodon, a GU wobble (at the third position of the codon) is also incorporated. Here, we observe not only the formation of additional H-bonds (i.e. enhanced tRNA:S9 interaction) but also loss of a non-Watson and Crick H-bond between the third G:U pair in the presence of the S9 tail.

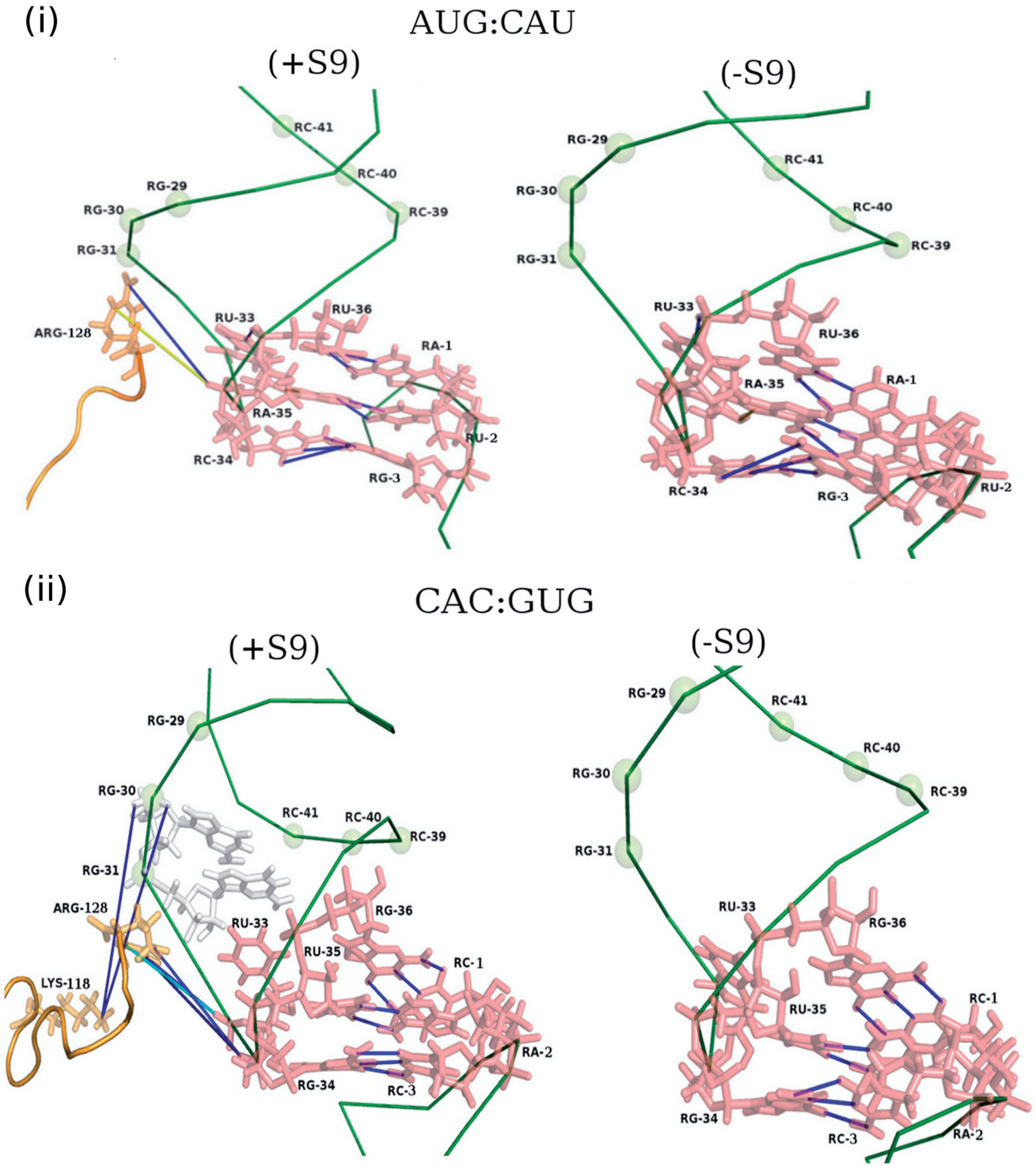

Figure 7. Pictorial representation of the dynamically stable H-bonds on the tRNA–mRNA and S9 complex from PDB accession number 2J00 in AUG:CAU (panel i), CAC:GUG (panel ii), CAU:GUG (panel iii) and AUC:GAU (panel iv) codon:anticodon pairs in the presence and absence of the S9 tail, respectively. The H-bonds present in 70% or more snapshots are depicted by blue line, whereas those in 60–70%, 50–60% and 40–50% of the snapshots are depicted by cyan, yellow and red lines, respectively. The $tRNA^{fMet}$ and mRNA backbones are depicted as deep green wires, and the residues of interest (both amino acids and nucleotides), participating in the H-bonds, are shown in stick representation.

(continued)

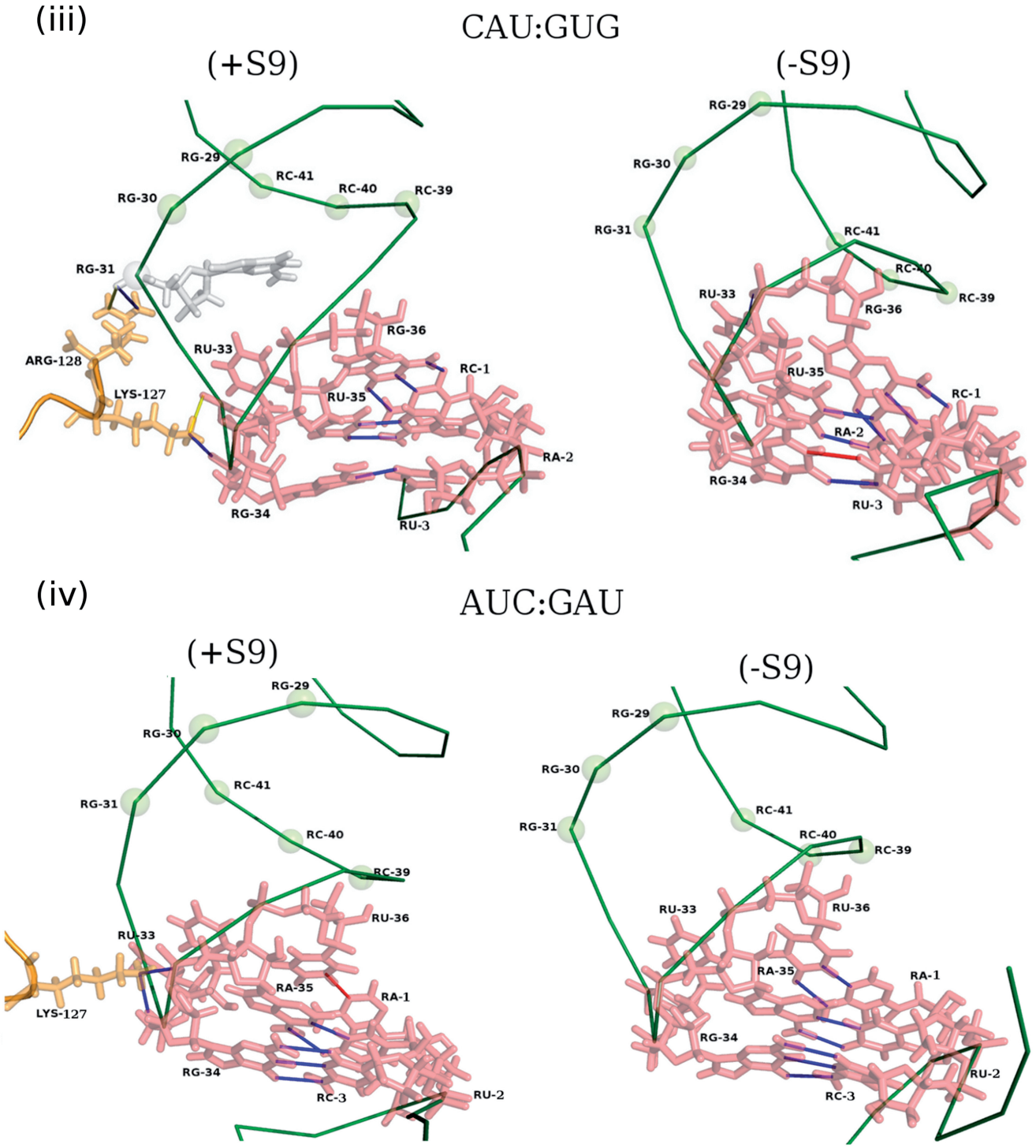

Figure 7. (Continued).

On deletion of the S9 tail, the lost H-bond between the G:U as also the dynamical properties of the system are regained, thus facilitating codon:anticodon pairing. These observations are in good agreement with the *in vivo* data showing an increase in initiation from CAC and CAU on S9 tail deletion (Figure 4).

Subsequently, as a control, we carried out MD simulations on the AUC:GAU codon:anticodon pair, which showed negligible change in initiation on S9 tail deletion (Figure 4). Interestingly, in this pair, S9 tail contacts position 33 and 34 of the tRNA (Figure 7, panel iv). The same contacts are seen for the wild-type $tRNA^{fMet}$ with the S9 tail. Thus, on deletion of the S9 tail, these contacts are lost without affecting the conformation of anticodon loop of tRNA or codon:anticodon interaction. It is, therefore, not surprising that initiation with the AUC:GAU pair is

not affected on deletion of the S9 tail. Also, the gain of the hydrogen bond at position 1 of the codon may compensate for the loss of the hydrogen bond made by the S9 tail with the positions 33/34 of the tRNA.

DISCUSSION

This study reveals the *in vivo* relevance of the methylated G966 and C967 and the C-terminal tail of the ribosomal protein S9 in the fidelity of decoding at the step of initiation. In a specific hypothesis, we propose that, to ensure fidelity of initiation, these elements (one or more) allow initiation from the authentic initiation codon (AUG), facilitate initiation from naturally used alternate initiation codons (such as GUG, UUG, CUG and so forth) and suppress initiation from unnatural initiation codons (such as CAC, CAU and so forth). Thus, in our approach, deletion of one or more of these elements (methylations at 966 or 967 positions and the S9 tail) would result in a minimal change in initiation from AUG, a decrease in initiation from the naturally used alternate initiation codons and an increase in initiation from the unnatural codons.

As seen for nearly all codon:anticodon pairs tested, initiation in the strain with a double deletion of the S9 tail and *rsmD* was not too different from that deleted for the S9 tail alone. Also, in most cases, fold changes in initiation were higher for a strain lacking S9 tail than the one lacking *rsmD*, suggesting a more pronounced effect of the S9 tail over the methylation at 966. We summarize our findings in Tables 1 and 2, and we discuss them as follows.

Methylated nucleosides G966 and C967 fine-tune initiation

A recent study showed that G966 and C967 methylations are important at an early step of initiation complex formation, and their lack led to ~2-fold decrease in binding of $tRNA^{fMet}$ (32). The importance of G966 in stabilizing elongator tRNAs at P-site has also been highlighted (33). In our study of their contributions in decoding at the P-site during initiation, we observed that the codon:anticodon pairs unnatural for initiation were discriminated against by these methylations. For example, deficiency of RsmB and/or RsmD resulted in increased initiation by $tRNA^{fMet}_{GUG}$ from CAC or CAU codons. Also, in our assays, where the native $tRNA^{fMet}_{CAU}$ was used to initiate from AUA codon, it initiated better in the absence of G966 methylation. We should mention that although the AUA:CAU pair with a CxA mismatch at the third position of the initiation codon is used as initiation codon in mitochondria, its use is facilitated by modification (formyl group) of the C34 of the CAU anticodon (3). In bacteria, where the anticodon of initiator tRNA is not modified, G966 methylation facing the CxA mismatch, may in fact be destabilizing. Interestingly, AUA decoding is special even at the step of elongation where C34 in $tRNA^{Ile}_{CAU}$ is modified with agmatidine in archea (34) and lysidine in eubacteria (35).

S9 tail contributes to the fidelity of initiation

The S9 C-terminal tail suppressed initiation with $tRNA^{fMet}_{GUG}$ using CAC and CAU codons, the pairs

Table 2. Summary of initiation activities (fold changes) of various anticodon stem mutants in the S9Δ3 strains expressed with respect to the parent *E. coli* SA

Anticodon in $tRNA^{fMet}$	Initiation codon in CAT	Anticodon stem mutation in $tRNA^{fMet}$	Fold changes in initiation in S9Δ3 strain w.r.t. the control (SA strain)
CUA	UAG	1GC (AU) mutant	1.37 ± 0.3
		1GC (GU) mutant	1.43 ± 0.3
		3GC mutant	2.3 ± 0.13
		2GC (AU/GU) mutant	3 ± 0.4
		No mutation in stem	1 ± 0.19

Table 1. Summary of initiation activities (fold changes) of various codon:anticodon combinations in the S9Δ3, Δ*rsmD* and S9Δ3 Δ*rsmD* strains expressed with respect to (w.r.t.) the parent *E. coli* SA

Anticodon in $tRNA^{fMet}$	Initiation codon in CAT	Fold changes in initiation in the given strain w.r.t. the control (SA strain)		
		S9Δ3	Δ*rsmD*	S9Δ3 Δ*rsmD*
GUG	CAC	2.5 ± 0.4	1.8 ± 0.1	2.5 ± 0.05
	CAU	3.8 ± 0.6	2.9 ± 0.3	4.5 ± 0.7
GUA	UAC	1 ± 0.03	1.52 ± 0.04	2 ± 0.26
GAU	AUC	1.1 ± 0.17	0.85 ± 0.08	0.96 ± 0.1
CUA	UAG	1 ± 0.2	1 ± 0.11	1 ± 0.19
CAU	AUG	1.14 ± 0.08	1.2 ± 0.09	1.17 ± 0.06
	GUG	0.6 ± 0.06	1.2 ± 0.3	0.67 ± 0.04
	UUG	0.47 ± 0.05	1.26 ± 0.04	0.63 ± 0.1
	CUG	0.76 ± 0.05	1.4 ± 0.02	0.9 ± 0.2
	AUA	1 ± 0.044	2 ± 0.02	1.35 ± 0.08
	AUU	0.83 ± 0.1	1.17 ± 0.25	1 ± 0.08
	AUC	0.98 ± 0.07	1.2 ± 0.15	0.95 ± 0.06
	ACG	1 ± 0.13	1 ± 0.02	1.2 ± 0.12

unnatural for initiation. Similarly, initiation by $tRNA^{fMet}_{GUA}$ was also prevented by the S9 tail. Essentially, in the absence of the S9 tail, G34 in place of C34 was accommodated better, which in turn led to better initiation. The S9 tail did not impact initiation with various other non-canonical codons (with mismatched first, second or the third positions of the codon) using the native initiator $tRNA^{fMet}_{CAU}$. However, initiation with the naturally used alternate initiation codons (UUG, GUG and CUG) decreased, suggesting that S9 facilitated stability of codon:anticodon interaction in these cases. Such a suggestion is supported by the MD simulations, which revealed that binding of $tRNA^{fMet}$ could be subtly affected on deletion of the S9 C-terminal tail (Figure 7). Although such an effect is unlikely to make a significant contribution (as a fraction towards the overall affinity) to a fully matched wild-type codon:anticodon pair (AUG:CAU), its contribution would mean more to a mismatched pair (such as in the cases of naturally used alternate initiation codons). Second, the binding of $tRNA^{fMet}$ was shown to decrease only modestly on S9 tail deletion (8). The modest decreases in the binding of $tRNA^{fMet}$ may become significant for initiation from UUG, GUG and CUG. In this context, an unexpected observation has been that the absence of the S9 tail did not impact initiation (using $tRNA^{fMet}_{CAU}$) even from the codons mismatched at their third positions.

Further, as revealed by the MD simulations (Figure 7, panels ii and iii), the regain of conformational dynamics and/or constrained hydrogen bond (between G:U pair) adequately explain increases in initiation from CAC and CAU codons by $tRNA^{fMet}_{GUG}$. The MD simulations also offered an explanation for negligible change in initiation with AUC:GAU pair (Figure 7, panel iv). Here, the H-bonds made between G34 of tRNA and the S9 tail are the same as reported for wild-type tRNA in the crystal structure (4). Thus, inspite of having G34 in its anticodon, this tRNA is largely insensitive to the presence or absence of the S9 tail. Finally, insights into the role of the S9 tail in decoding during initiation were gained by analysis of initiation with the 3GC variants of $tRNA^{fMet}$ where the mutants lacking either 2GC or all 3GC base pairs initiated significantly better in the absence of the S9 tail. This observation contrasted the earlier report (8), where the elongator tRNAs ($tRNA^{Phe}$, $tRNA^{Cys}$) having 2GC base pairs in the anticodon stem were preferentially stabilized in the absence of S9 tail. This may be explained by the fact that the *in vitro* study (8) did not use IF3, whereas in the *in vivo* context, IF3 would have a role to play in discriminating against the initiator tRNAs lacking the three GC pairs (36).

Interestingly, the S9 tail phenocopies the role of IF3 in discriminating against tRNAs lacking the 3GC base pairs (36), suggesting that the S9 tail and IF3 may function in concert. The two key roles of IF3 are to discriminate start codons AUG, GUG and UUG from the rest and to discriminate initiator tRNA via its 3GC base pairs. On deletion of the S9 tail both the functions are affected, suggesting that the deletion of the S9 tail has effects in common with the deficiency of IF3; it would be of future interest to investigate these mechanisms further.

P-site ribosomal proteins and the initiator tRNA

This study highlights the functional/evolutionarily important roles that the proteins located within the ribosomal P-site may have. It also rationalizes the selection and conservation of the anticodon of the initiator tRNA. Initiator tRNA has a conserved C34 in its anticodon, which seems to be important for the ribosome to distinguish it from other tRNAs, allowing its selection from a pool of tRNAs richly populated by elongators. This process is facilitated by the P-site features, such as the methylated G966 and the S9 tail of the ribosome. The 3GC base pairs too are important in the process of selective targeting of the initiator tRNA to the P-site. However, the interactions between P-site features and the initiator tRNA seem complex and specific for various codon:anticodon interactions.

SUPPLEMENTARY DATA

Supplementary Data are available at NAR Online: Supplementary Tables 1–7, Supplementary Figures 1–8, Supplementary Methods, Supplementary Results and Discussion and Supplementary References [37–45].

ACKNOWLEDGEMENTS

The authors thank their laboratory colleagues for their suggestions on the manuscript. U.V. is a J. C. Bose fellow of DST. S.V. is an Emeritus Scientist, and S.A. was a senior research fellow of the Council of Scientific and Industrial Research, New Delhi.

FUNDING

Departments of Science and Technology (DST), and Biotechnology (DBT), New Delhi. Funding for open access charge: DBT and DST.

Conflict of interest statement. None declared.

REFERENCES

1. Ogle,J.M., Brodersen,D.E., Clemons,W.M. Jr, Tarry,M.J., Carter,A.P. and Ramakrishnan,V. (2001) Recognition of cognate transfer RNA by the 30S ribosomal subunit. *Science*, **292**, 897–902.
2. Sacerdot,C., Chiaruttini,C., Engst,K., Graffe,M., Milet,M., Mathy,N., Dondon,J. and Springer,M. (1996) The role of the AUU initiation codon in the negative feedback regulation of the gene for translation initiation factor IF3 in Escherichia coli. *Mol. Microbiol.*, **21**, 331–346.
3. Takemoto,C., Spremulli,L.L., Benkowski,L.A., Ueda,T., Yokogawa,T. and Watanabe,K. (2009) Unconventional decoding of the AUA codon as methionine by mitochondrial tRNAMet with the anticodon f5CAU as revealed with a mitochondrial in vitro translation system. *Nucleic Acids Res.*, **37**, 1616–1627.
4. Selmer,M., Dunham,C.M., Murphy,F.V. IV, Weixlbaumer,A., Petry,S., Kelley,A.C., Weir,J.R. and Ramakrishnan,V. (2006) Structure of the 70S ribosome complexed with mRNA and tRNA. *Science*, **313**, 1935–1942.
5. Dunkle,J.A., Wang,L., Feldman,M.B., Pulk,A., Chen,V.B., Kapral,G.J., Noeske,J., Richardson,J.S., Blanchard,S.C. and Cate,J.H. (2011) Structures of the bacterial ribosome in classical and hybrid states of tRNA binding. *Science*, **332**, 981–984.

6. Lesnyak,D.V., Osipiuk,J., Skarina,T., Sergiev,P.V., Bogdanov,A.A., Edwards,A., Savchenko,A., Joachimiak,A. and Dontsova,O.A. (2007) Methyltransferase that modifies guanine 966 of the 16 S rRNA: functional identification and tertiary structure. *J. Biol. Chem.*, **282**, 5880–5887.
7. Gu,X.R., Gustafsson,C., Ku,J., Yu,M. and Santi,D.V. (1999) Identification of the 16S rRNA m5C967 methyltransferase from Escherichia coli. *Biochemistry*, **38**, 4053–4057.
8. Hoang,L., Fredrick,K. and Noller,H.F. (2004) Creating ribosomes with an all-RNA 30S subunit P site. *Proc. Natl Acad. Sci. USA*, **101**, 12439–12443.
9. Maden,B.E. (1990) The numerous modified nucleotides in eukaryotic ribosomal RNA. *Prog. Nucleic Acid Res. Mol. Biol.*, **39**, 241–303.
10. Kowalak,J.A., Bruenger,E., Crain,P.F. and McCloskey,J.A. (2000) Identities and phylogenetic comparisons of posttranscriptional modifications in 16 S ribosomal RNA from Haloferax volcanii. *J. Biol. Chem.*, **275**, 24484–24489.
11. Saraiya,A.A., Lamichhane,T.N., Chow,C.S., SantaLucia,J.Jr. and Cunningham,P.R. (2008) Identification and role of functionally important motifs in the 970 loop of *Escherichia coli* 16S ribosomal RNA. *J. Mol. Biol.*, **376**, 645–657.
12. Aduri,R., Psciuk,B.T., Saro,P., Taniga,H., Schlegel,H.B. and SantaLucia,J. (2007) AMBER force field parameters for the naturally occurring modified nucleosides in RNA. *J. Chem. Theory Comput.*, **3**, 1464–1475.
13. Brodersen,D.E., Clemons,W.M. Jr, Carter,A.P., Wimberly,B.T. and Ramakrishnan,V. (2002) Crystal structure of the 30 S ribosomal subunit from *Thermus thermophilus*: structure of the proteins and their interactions with 16 S RNA. *J. Mol. Biol.*, **316**, 725–768.
14. Das,G., Thotala,D.K., Kapoor,S., Karunanithi,S., Thakur,S.S., Singh,N.S. and Varshney,U. (2008) Role of 16S ribosomal RNA methylations in translation initiation in *Escherichia coli*. *EMBO J.*, **27**, 840–851.
15. Seshadri,A., Dubey,B., Weber,M.H.W. and Varshney,U. (2009) Impact of rRNA methylations on ribosome recycling and fidelity of initiation in *Escherichia coli*. *Mol. Microbiol.*, **72**, 795–808.
16. Osterman,I.A., Sergiev,P.V., Tsvetkov,P.O., Makarov,A.A., Bogdanov,A.A. and Dontsova,O.A. (2011) Methylated 23S rRNA nucleotide m2G1835 of *Escherichia coli* ribosome facilitates subunit association. *Biochimie*, **93**, 725–729.
17. Connolly,K., Rife,J.P. and Culver,G. (2008) Mechanistic insight into the ribosome biogenesis functions of the ancient protein KsgA. *Mol. Microbiol.*, **70**, 1062–1075.
18. Vazquez-Laslop,N., Ramu,H., Klepacki,D., Kannan,K. and Mankin,A.S. (2010) The key function of a conserved and modified rRNA residue in the ribosomal response to the nascent peptide. *EMBO J.*, **29**, 3108–3117.
19. Varshney,U. and RajBhandary,U.L. (1990) Initiation of protein synthesis from a termination codon. *Proc. Natl Acad. Sci. USA*, **87**, 1586–1590.
20. Zheng,G., Lu,X.J. and Olson,W.K. (2009) Web 3DNA–a web server for the analysis, reconstruction, and visualization of three-dimensional nucleic-acid structures. *Nucleic Acids Res.*, **37**, W240–W246.
21. Case,D.A., Darden,T.A., Cheatham,T.E. III, Simmerling,C.L., Wang,J., Duke,R.E., Luo,R., Merz,K.M., Pearlman,D.A., Crowley,M. *et al.* (2006) AMBER 9, University of California, San Francisco.
22. Varshney,U., Lee,C.P., Seong,B.L. and RajBhandary,U.L. (1991) Mutants of initiator tRNA that function both as initiators and elongators. *J. Biol. Chem.*, **266**, 18018–18024.
23. Kapoor,S., Das,G. and Varshney,U. (2011) Crucial contribution of the multiple copies of the initiator tRNA genes in the fidelity of tRNA(fMet) selection on the ribosomal P-site in Escherichia coli. *Nucleic Acids Res.*, **39**, 202–212.
24. Schulman,L.H. and Goddard,J.P. (1973) Loss of methionine acceptor activity resulting from a base change in the anticodon of *Escherichia coli* formylmethionine transfer ribonucleic acid. *J. Biol. Chem.*, **248**, 1341–1345.
25. Giege,R., Sissler,M. and Florentz,C. (1998) Universal rules and idiosyncratic features in tRNA identity. *Nucleic Acids Res.*, **26**, 5017–5035.
26. Mayer,C., Kohrer,C., Kenny,E., Prusko,C. and RajBhandary,U.L. (2003) Anticodon sequence mutants of *Escherichia coli* initiator tRNA: effects of overproduction of aminoacyl-tRNA synthetases, methionyl-tRNA formyltransferase, and initiation factor 2 on activity in initiation. *Biochemistry*, **42**, 4787–4799.
27. Harada,F. and Nishimura,S. (1972) Possible anticodon sequences of tRNA His, tRNA Asm, and tRNA Asp from *Escherichia coli* B. Universal presence of nucleoside Q in the first postion of the anticondons of these transfer ribonucleic acids. *Biochemistry*, **11**, 301–308.
28. Gold,L. (1988) Posttranscriptional regulatory mechanisms in *Escherichia coli*. *Annu. Rev. Biochem.*, **57**, 199–233.
29. Childs,J., Villanueba,K., Barrick,D., Schneider,T.D., Stormo,G.D., Gold,L., Leitner,M. and Caruthers,M. (1985) Ribosome binding site sequences and function. In: Calendar,R. and Gold,L. (eds), *Sequence Specificity in Transcription and Translation*. Alan R. Liss, New York, NY, pp. 341–350.
30. Shinedling,S., Gayle,M., Pribnow,D. and Gold,L. (1987) Mutations affecting translation of the bacteriophage T4 rIIB gene cloned in Escherichia coli. *Mol. Gen. Genet.*, **207**, 224–232.
31. Mandal,N., Mangroo,D., Dalluge,J.J., McCloskey,J.A. and Rajbhandary,U.L. (1996) Role of the three consecutive G:C base pairs conserved in the anticodon stem of initiator tRNAs in initiation of protein synthesis in *Escherichia coli*. *RNA*, **2**, 473–482.
32. Burakovsky,D.E., Prokhorova,I.V., Sergiev,P.V., Milon,P., Sergeeva,O.V., Bogdanov,A.A., Rodnina,M.V. and Dontsova,O.A. (2012) Impact of methylations of m2G966/m5C967 in 16S rRNA on bacterial fitness and translation initiation. *Nucleic Acids Res.*, **40**, 7885–7895.
33. Shoji,S., Abdi,N.M., Bundschuh,R. and Fredrick,K. (2009) Contribution of ribosomal residues to P-site tRNA binding. *Nucleic Acids Res.*, **37**, 4033–4042.
34. Ikeuchi,Y., Kimura,S., Numata,T., Nakamura,D., Yokogawa,T., Ogata,T., Wada,T. and Suzuki,T. (2010) Agmatine-conjugated cytidine in a tRNA anticodon is essential for AUA decoding in archaea. *Nat. Chem. Biol.*, **6**, 277–282.
35. Grosjean,H. and Bjork,G.R. (2004) Enzymatic conversion of cytidine to lysidine in anticodon of bacterial isoleucyl-tRNA–an alternative way of RNA editing. *Trends Biochem. Sci.*, **29**, 165–168.
36. O'Connor,M., Gregory,S.T., Rajbhandary,U.L. and Dahlberg,A.E. (2001) Altered discrimination of start codons and initiator tRNAs by mutant initiation factor 3. *RNA*, **7**, 969–978.
37. Datsenko,K.A. and Wanner,B.L. (2000) One-step inactivation of chromosomal genes in *Escherichia coli* K-12 using PCR products. *Proc. Natl Acad. Sci. USA*, **97**, 6640–6645.
38. Miller,J.H. (1972) *In Experiments in Molecular Genetics*. Cold Spring Harbour Laboratory, Cold Spring Harbour, NY.
39. Baba,T., Ara,T., Hasegawa,M., Takai,Y., Okumura,Y., Baba,M., Datsenko,K.A., Tomita,M., Wanner,B.L. and Mori,H. (2006) Construction of *Escherichia coli* K-12 in-frame, single-gene knockout mutants: the Keio collection. *Mol. Syst. Biol.*, **2**, 2006.0008.
40. Varshney,U., Lee,C.P. and RajBhandary,U.L. (1991) Direct analysis of aminoacylation levels of tRNAs in vivo. Application to studying recognition of *Escherichia coli* initiator tRNA mutants by glutaminyl-tRNA synthetase. *J. Biol. Chem.*, **266**, 24712–24718.
41. Pomerantz,S.C. and McCloskey,J.A. (1990) Analysis of RNA hydrolyzates by liquid chromatography-mass spectrometry. *Methods Enzymol.*, **193**, 796–824.
42. Pallanck,L. and Schulman,L.H. (1991) Anticodon-dependent aminoacylation of a noncognate tRNA with isoleucine, valine, and phenylalanine *in vivo*. *Proc. Natl Acad. Sci. USA*, **88**, 3872–3876.
43. Lee,C., Yu,D., Velasco,M., Tessarollo,L., Swing,D.A., Court,D.L., Jenkins,N.A. and Copeland,N.G. (2001) A highly efficient *Escherichia coli*-based chromosome engineering system adapted for recombinogenic targeting and subcloning of BAC DNA. *Genomics*, **73**, 56–65.
44. Samhita,L., Shetty,S. and Varshney,U. (2012) Unconventional initiator tRNAs sustain Escherichia coli. *Proc. Natl Acad. Sci. USA*, **109**, 13058–13063.
45. Cherepanov,P.P. and Wackernagel,W. (1995) Gene disruption in *Escherichia coli*: TcR and KmR cassettes with the option of Flp-catalyzed excision of the antibiotic-resistance determinant. *Gene*, **158**, 9–14.